applied sciences

MDPI

Article

High-Performance Lead-Acid Batteries Enabled by Pb and PbO_2 Nanostructured Electrodes: Effect of Operating Temperature

Roberto Luigi Oliveri, Maria Grazia Insinga, Simone Pisana, Bernardo Patella, Giuseppe Aiello and Rosalinda Inguanta *

Laboratorio di Chimica Fisica Applicata, Dipartimento di Ingegneria, Università di Palermo, Viale delle Scienze, Ed. 6, 90128 Palermo, Italy; robertoluigi.oliveri@unipa.it (R.L.O.); mariagrazia.insinga@unipa.it (M.G.I.); SimonePisana@hotmail.it (S.P.); bernardo.patella@unipa.it (B.P.); giuseppe.aiello03@unipa.it (G.A.)
* Correspondence: rosalinda.inguanta@unipa.it

Abstract: Lead-acid batteries are now widely used for energy storage, as result of an established and reliable technology. In the last decade, several studies have been carried out to improve the performance of this type of batteries, with the main objective to replace the conventional plates with innovative electrodes with improved stability, increased capacity and a larger active surface. Such studies ultimately aim to improve the kinetics of electrochemical conversion reactions at the electrode-solution interface and to guarantee a good electrical continuity during the repeated charge/discharge cycles. To achieve these objectives, our contribution focuses on the employment of nanostructured electrodes. In particular, we have obtained nanostructured electrodes in Pb and PbO_2 through electrosynthesis in a template consisting of a nanoporous polycarbonate membrane. These electrodes are characterized by a wider active surface area, which allows for a better use of the active material, and for a consequent increased specific energy compared to traditional batteries. In this research, the performance of lead-acid batteries with nanostructured electrodes was studied at 10 C at temperatures of 25, −20 and 40 °C in order to evaluate the efficiency and the effect of temperature on electrode morphology. The batteries were assembled using both nanostructured electrodes and an AGM-type separator used in commercial batteries.

Keywords: lead nanowires; template electrodeposition; lead-acid battery; nanostructures cycling efficiency; high C-rate cycling; temperature test

Citation: Oliveri, R.L.; Insinga, M.G.; Pisana, S.; Patella, B.; Aiello, G.; Inguanta, R. High-Performance Lead-Acid Batteries Enabled by Pb and PbO_2 Nanostructured Electrodes: Effect of Operating Temperature. *Appl. Sci.* **2021**, *11*, 6357. https://doi.org/10.3390/app11146357

Academic Editor: Dong-Won Kim

Received: 15 June 2021
Accepted: 7 July 2021
Published: 9 July 2021

1. Introduction

Improving the efficiency of energy recovery processes in relevant applications, such as the regenerative braking in vehicles, elevators and cranes, requires energy storage devices that enable faster charging and discharging compared to existing lithium-ion batteries, which are the highest energy density batteries currently available on the market [1]. Capacitors are also able to charge and discharge much faster than existing batteries, performing hundreds of thousands of charge/discharge cycles without significant loss of capacity. However, the energy storage density of capacitors is generally significantly lower compared to batteries. Lead batteries include three essential elements: sulfuric acid, used as an electrolyte, and lead and lead dioxide, used as a negative and a positive electrode. Each cell is able to supply a voltage of about 2 volts, while the current is a function of the electrode surface. The electrode surface is thus the characterizing element of this device, and several studies can be found in the literature, discussing possible solutions to obtain electrodes with a high active surface, thus improving the reactions occurring at the electrode-electrolyte interface, in order to ensure electrical continuity and an increased number of charge/discharge cycles. However, due to the low specific energy storage of these devices (about 30–40 Whg^{-1}), compared to other batteries, and considering that current lead-acid batteries work in optimal conditions at a maximum discharge current (C-rate) of C/5 [2], their application is limited in advanced systems. In addition, due to

the high atomic weight of lead, such batteries are characterized by a low specific energy and, consequently, by a high battery weight. Another relevant drawback is related to the low utilization degree of active pastes. In fact, during the charge/discharge cycles, the active pastes are subject to the desulphation-sulphation reactions. In particular, during discharge, there is the formation of large and non-conductive $PbSO_4$ crystals, both in the positive and negative plate, which progressively reduce the active surface [3]. Moreover, the continuous volume variations due to the sulphation/desulphation reactions cause the mechanical instability of the plates, which causes a progressive deterioration and a gradual loss of capacity [4].

Lead-acid batteries are thus less competitive than other rechargeable batteries. Different studies have been conducted over the years to improve the performance of lead batteries, to increase the number of life cycles, to increase their energy density and to decrease sulphation phenomena. The approaches currently employed in such regard involve the use of additives, such as different types of carbon powder, carbon nanotubes, titanium dioxide, glass fibers, silicon dioxide and aluminum oxide [5], carboxes [6] and graphene [7]. Lankipalli et al. [8] studied the effect of adding TiO_2 in the positive active material (PAM) and carbon nanostructures on the negative active material (NAM), obtaining small tetrabasic sulfate crystals that increase the exposed active surface area and thus achieve longer battery life and capacity by retarding sulfate formation. Aleksandrova et al. [9] also achieved improved cycle life (up to 3600 cycles) and increased the overvoltage of hydrogen evolution under high-rate partial state-of-charge conditions (HRPSoC) by adding ZnO and nanocarbon in the NAM. Another peculiarity of these batteries is that their performance is highly dependent on temperature. In their studies, in fact, the authors achieved an excellent efficiency at high temperature due to kinetic reasons, but nevertheless, with each 8 °C increase in temperature, they reported a reduction of the battery life by up to half [10]. Moreover, when the temperature decreases, the electrolyte becomes more and more viscous, thus allowing the delay of $PbSO_4$ formation, which, combined with the efficiency decrease due to the low temperature, leads to the freezing of the container, which can cause damage to the plates [11].

Therefore, although lead-acid battery (LAB) is the oldest electrochemical energy storage system, its diffusion in new and emerging sectors of technological interest is inhibited by its negative aspects. To overcome these problems, and considering that the electrochemical reactions inside the cell take place mainly on the active surface of the electrode, which is exposed to the electrolyte, a promising solution to improve the performance of lead-acid batteries is to replace conventional electrode plates with innovative electrodes made of nanostructured active materials, that ensure both a high surface area and greater accessibility of the electrolyte within the active material.

This research aims at maximizing the surface area of the LAB electrodes to optimize the utilization of the active material present in the cell, therefore enhancing the performance of lead accumulators, and obtaining a competitive device in areas where other technologies (e.g., lithium batteries and supercapacitors) are commonly used.

An important battery requirement, in addition to high specific energy, is long lifetime under continuous cycling at HRPSoC owing to the intermittent operation for applications, such as in Full Electric Vehicles (EVs), where the weight also matters. Such a requirement today is fully satisfied by Li-ion batteries, which are, however, unsafe, and currently highly expensive [12,13]. For off-grid applications and renewable energy storage that is stationary in nature, the weight of the battery is unimportant. In these fields, there is a great opportunity for batteries alternative to lithium-ion that use abundant raw materials. Specifically, zinc-ion rechargeable batteries have recently received much attention owing to the high abundance of zinc in natural resources, intrinsic safety and cost, when compared with the lithium-ion batteries. Attempts to develop rechargeable aqueous zinc-ion batteries (ZIBs) can be traced to as early as the 1980s; however, since 2015, the research activity in this field has surged throughout the world. Despite the achievements made in exploring electrode materials so far, significant challenges remain at the material level and even on

the whole aqueous ZIBs system [14–16]. In this context, LABs are still a valid alternative, and the possibility of optimizing their performance in terms of energy density and rate of charge and discharge is still an interesting solution for the medium term.

The subject dealing with the lead-acid battery performance at HRPSoC has been extensively investigated, and different solutions were proposed, such as modifying the negative active material composition through suitable additives, designing innovative assembly with a super-capacitor or improving the energy efficiency through proper managing of the charging process [17–21]. The ultimate goal is to increase the energy density in order to enhance the performance of lead-acid batteries. These goals can be achieved thanks to the use of polycarbonate membranes with interconnected pores, that permit to realize nanostructured Pb and PbO_2 electrodes, through the template electrodeposition method, that are characterized by a very high active surface.

In our previous works, these types of nanostructured electrodes have been tested, obtaining excellent results [12,22,23]. In this work, we show some preliminary results obtained from tests carried out on nanostructured electrodes at different temperatures. In particular, we will show that they are able to work, even under stress conditions, at high charge/discharge rates (from 1 to 10 C) and at temperatures from −20 to 40 °C.

2. Materials and Methods

In previous works [4,12,22,23], we have illustrated how to grow PbO_2 and Pb nanowires (NWs) by electrodeposition in Whatman polycarbonate (PC) membrane (Cytiva, Marlborough, MA, USA) 47, which was used as a template allowing to obtain a morphology in the nanowire shape. The template electrodeposition method consists of different steps. The first step is the sputtering process, necessary to make the membrane conductive. Then, a current collector is deposited, which acts as a mechanical support and electrical contact for the nanostructures. Finally, the growth of the nanostructures takes place inside the pores of the template. The obtained morphology, therefore, is intimately related to the template used and is shown in Figure 1, for the PbO_2 nanostructured electrode in addition to the template used.

In detail, in the first step, a uniform and thick layer of PbO_2 was electrodeposited onto the Au-coated side of the membrane at room temperature under a constant current of 10 mA cm^2, up to a charge of 80 C cm^2. In the second step, PbO_2 nanowires were grown inside membrane channels at 60 °C, applying a constant potential of 1.5 V vs. Saturated Calomel Electrode (SCE), up to 8 C cm^2.

Both electrodepositions were performed from an aqueous solution of 1 M $Pb(NO_3)_2$ (Sigma, 99%) and 0.3 M $H(NO)_3$ (Sigma, 70%). For the electrodeposition of Pb current collector and NWs, a solution of 4.5 g/L $C_{20}H_{26}O_{10}S_2$ (Sigma, 99%), 15 g/L H_3BO_3 (Sigma, 99%), 35.2 g/L HBF_4 (Sigma, 48%) and 40.9 g/L $Pb(BF_4)_2$ (Sigma, 50%) was employed, applying a pulse current deposition at room temperature.

The current collector was obtained through three steps, each 960 s long. The solution was replaced at the end of each step for avoiding the degradation effects and improving the deposition quality. NW growth was carried out in a single step of 330 s. Electrodeposition of both NWs and current collectors was performed with a PAR Potentiostat/Galvanostat (mod. PARSTAT 2273, Princeton Applied Research, TN, USA) connected to a PC and controlled by POWERSUITE® software (Princeton Applied Research, TN, USA).

After electrodeposition, the polycarbonate membrane was dissolved in $CHCl_3$ to obtain a nanostructured electrode consisting of a nanowire array electrically connected to the current collector. A scheme of the nanostructured electrode after the fabrication process is shown in Figure 2.

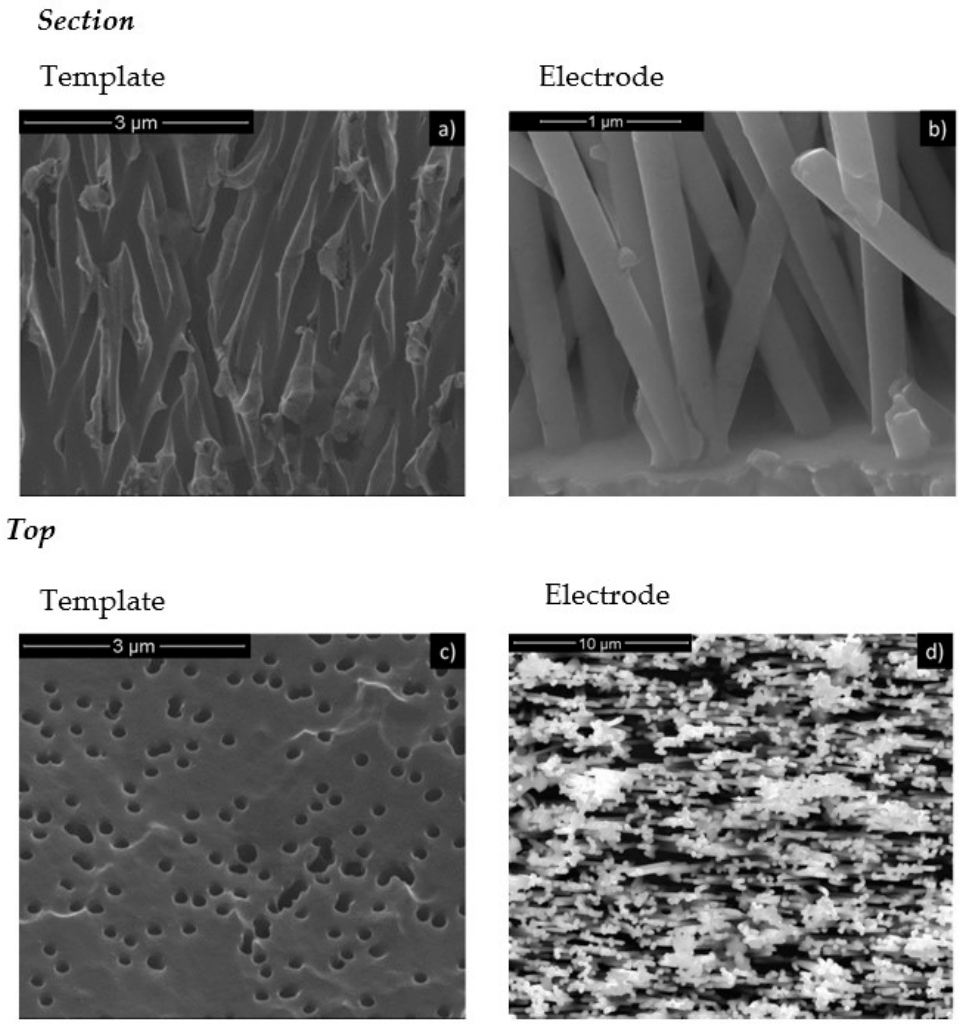

Figure 1. Scanning electron microscope (SEM) images of the polycarbonate (PC) membrane (**a**,**c**) and nanostructures (**b**,**d**): (**a**,**b**) cross-sectional view and (**c**,**d**) top view.

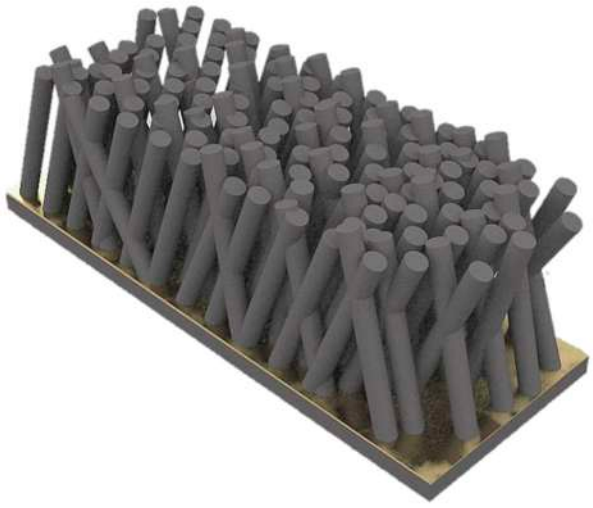

Figure 2. Scheme of the nanostructured electrode.

The active mass of nanowires was evaluated by gravimetric measurements using a Sartorius microbalance (mod. Premium Microbalance ME36S, Sartorius, Germany). The loading of the PbO_2 and Pb NWs on the current collector was 6.16 ± 0.5 and 3.84 ± 0.3 mg/cm^2,

respectively. The gravimetric capacity of Pb is higher than PbO_2, so that the performance of the nanostructured lead-acid cell was controlled by PbO_2. NWs characterization was carried out by X-ray diffraction (XRD), Energy Dispersive X-ray Spectrometry (EDS) and Scanning Electron Microscopy (SEM). In particular, to investigate the morphology and the atomic composition of the nanostructured electrode, a FEG-ESEM FEI (mod. QUANTA 200, FEI, OR, USA), equipped with an Energy Dispersive Spectroscopy (EDS, EDAX) probe, was used. An X-ray diffractometer (mod. D-MAX 25,600 HK, Rigaku, Tokyo, Japan) was employed for XRD analyses. More details can be found in [24–28]. Charge/discharge cycles were carried out by means of a multi-channel cell test system (Solartron, 1470E, Ametek, PA, USA) at different temperatures. Data were acquired and processed by using MULTISTAT® and CorrView® software (Ametek, PA, USA), respectively.

3. Results and Discussion

A separate study of nanostructured lead and lead oxide electrodes is reported in [4,12]. The cell presented in this work consists of both nanostructured electrodes. In particular, the battery used for testing consists of a nanostructured PbO_2 electrode with a geometric area of about 1.1 cm^2, a nanostructured Pb electrode with a geometric area of about 7.1 cm^2, a commercial Absorptive Glass Mat separator (AGM) and a 5 M sulfuric acid aqueous solution as the electrolyte. Figure 3 shows a 3D scheme of the nanostructured battery. The nanostructured electrodes were assembled with zero gap configuration to simulate the similar condition of a commercial lead-acid battery, and tested at a C-rate from 1 to 30 C with a cut-off of 1.2 V. These are very stressing conditions in comparison to conventional working conditions of a commercial lead-acid battery. The lead oxide electrode was previously immersed in 5 M sulfuric acid before testing. This step is necessary to overcome its low wettability and avoid an initial high potential value that may result in electrode failure.

The active mass of the nanowires used to evaluate the nominal capacity of the electrodes was evaluated by gravimetric measurements using a microbalance. Specifically, the electrochemical tests were based on the gravimetric capacitance of PbO_2 since the positive electrode was limiting compared to the negative Pb electrode due to the smaller size of the geometric surface area. Electrochemical tests were performed in two steps. First, conditioning of the nanostructured cells at 1 C was performed. After pre-soaking, the battery was subjected to an initial charge. This charge, which is conducted according to a previously predicted multi-step current procedure [4] which consists of a gradual increase in current from C/5 up to 1 C, plays a crucial role for the mechanical stability of the nanostructured electrodes. In fact, during this step, the cell voltage drops very slowly, avoiding the formation of hydrogen and oxygen that can damage the nanostructures. In particular, this procedure was optimized to keep the cell voltage below 3 V to avoid gas evolution, which would cause mechanical stress to the electrodes and the transportation of acidic drops to the metal parts, causing their corrosion. At the end of this charge, the nanostructured electrodes were cycled at 1 C for 100 cycles and at 25 °C. This is the conditioning phase of the nanostructured lead-acid electrodes and is necessary for electrode stabilization.

The conditioning step was followed by an electron microscopic analysis using Scanning Electron Microscope to evaluate the change in electrode morphology. This analysis was performed because improved battery performance with nanostructured electrodes is associated with improved wettability of the porous mass of the nanostructured electrodes. This behavior is well-known as a peculiarity of lead-acid batteries [29,30]. In Figure 3, we showed the morphology displayed by a PbO_2 electrode before and after the conditioning step.

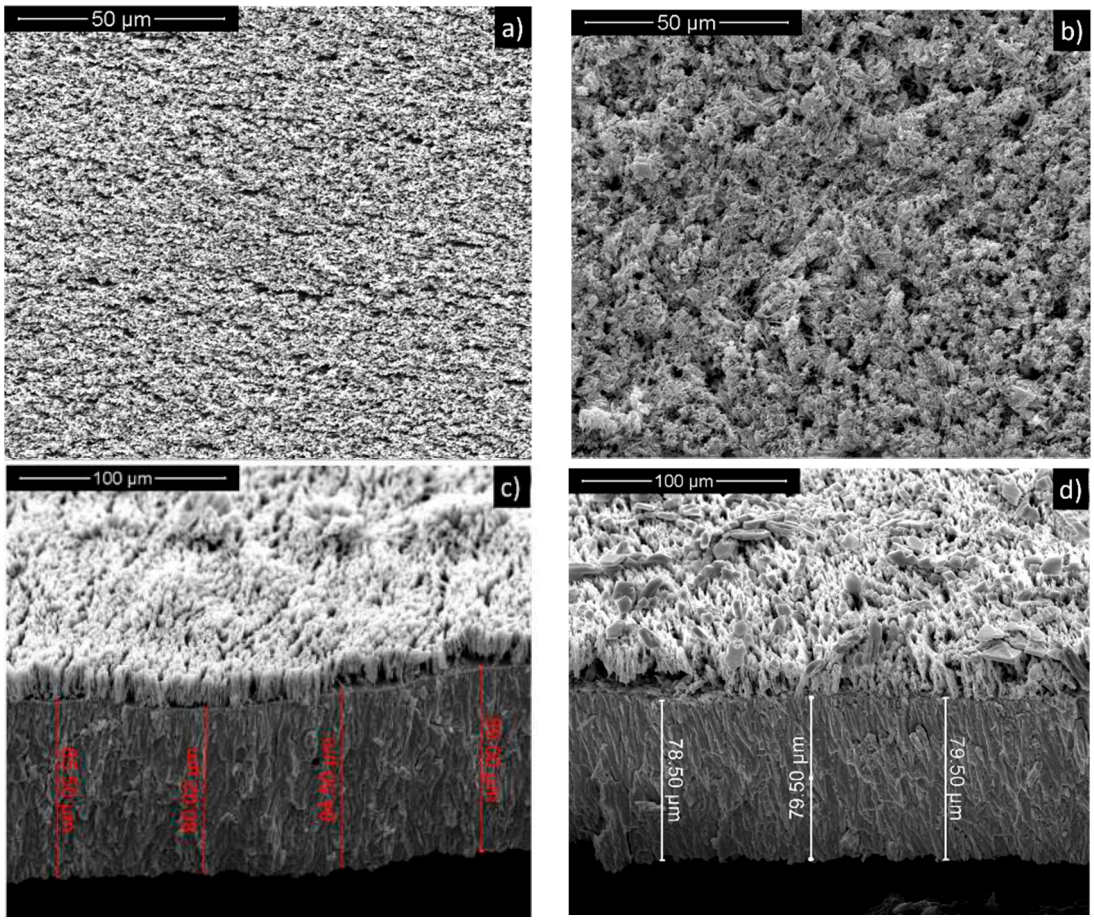

Figure 3. SEM images of PbO_2 NW electrode: (**a**) top view before the conditioning phase, (**b**) top view after the conditioning phase, (**c**) cross-sectional view before the conditioning phase and (**d**) cross-sectional view after the conditioning phase.

In detail, Figure 3a,c shows the initial top and cross-sectional view morphology of the lead oxide electrode, consisting of many nanowires that cover the overall surface of the electrode, and cavities that allow the electrolyte (H_2SO_4 5 M) to penetrate and encounter a larger active surface for the charge/discharge reactions of the battery. On the other hand, in Figure 3b,d, the micrographs shown are related to the morphology of the electrode after the conditioning phase, lasting 100 cycles. In particular, in Figure 3d, the cross-sectional view of the electrode was reported, which highlights both the top of the electrode, in which the nanowires are present, and the current collector. It is important to highlight that the collector appears perfectly intact, with an identical morphology to the as-prepared one, indicating that it does not fully participate in the charge and discharge reactions that only the nanowires undergo. Figure 3b shows a morphology almost close to the initial one, where the nanowires are still evident, although they have a more pronounced roughness. In addition, lead sulfate microcrystals are also visible on the electrode surface. Based on these results, it can be concluded that nanostructures formed by template electrodeposition change their morphology during the cyclization, generating in situ a porosity that cannot be obtained by other methods. In addition, the increase in volume during discharge does not interrupt the electrolytic continuity between the active electrode material and the current collector, providing a high degree of utilization of the active material. This is perhaps the biggest difference from commercial plates, where the volume increase associated with the conversion reaction interrupts electrolytic continuity between the current grid and the far regions, lowering the degree of utilization of the active material by up to 50%, with associated performance consequences. To limit these problems, commercial plates are cycled at low speeds.

On the Pb NW electrode, after the post-conditioning step, in particular at the end of the 100th discharge, a quantitative XRD analysis was performed to determine the amount of lead and lead sulfate present in the electrode. Figure 4 shows the result of this analysis. As expected, for an almost fully discharged electrode, $PbSO_4$ is almost 98.9%, while Pb is 1.1%.

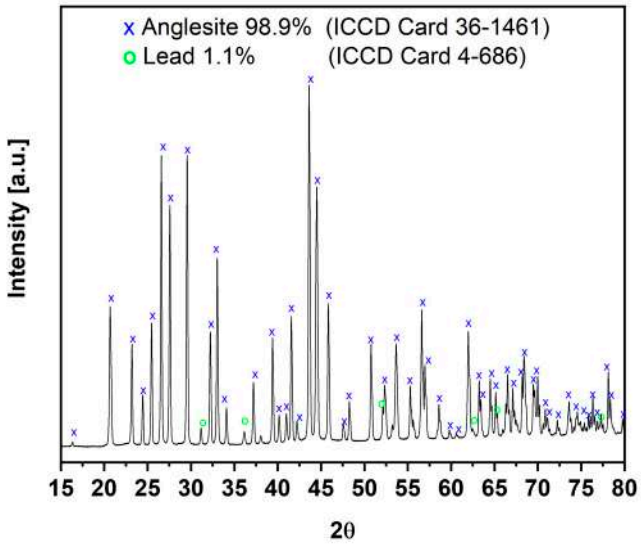

Figure 4. X-ray diffraction (XRD) pattern of Pb NW electrode after conditioning phase and at the end of the 100th discharge.

After the conditioning step, the nanostructured electrodes were tested at different temperatures. Operating temperature is a very important factor for lead-acid batteries and can strongly influence their performance. For example, it has been observed that at high temperatures, internal resistances decrease and reaction kinetics occurring at the electrodes are favored, resulting in an increased capacity and higher energy delivered. However, high temperatures also facilitate self-discharge processes and the consequent capacity loss. If the kinetics is favored at high temperatures, it is disadvantaged at low temperatures. The reactions of the cells slow down, but in spite of this, in the charging phase, it is possible to obtain a final microporous morphology of the electrode (so a very large active surface) that allows to optimize the performance. In this work, nanostructured lead-acid electrodes were tested at 25, −20 and 40 °C, the last two being the critical temperatures for a lead-acid battery according to EN 61427-1:2013 [31], at which commercial electrodes are normally tested in order to ensure good performance even at critical temperatures. In this case, the nanostructured electrodes were tested at a C-rate of 10 C, which means charging/discharging the battery in 6 min, with a cut-off of 1.2 V and a discharge rate of 90% of the charge. A number of charge/discharge cycles of 1000 was set for these tests.

After the conditioning phase, an initial test was performed at a temperature of 25 ± 2 °C. Figure 5a shows the charging and discharging curves of the battery, while Figure 5b displays the discharge capacity and the efficiency of the nanostructured battery.

Figure 5a shows a strong polarization of the electrodes in the first 50 cycles, which decreases with cyclization. The charge curves do not show peaks, meaning that there is a very limited gas development on the electrodes' surface despite the high cyclization rate. The discharge curves show an increase of the plateau with cyclization, which means an increase of usable energy of the battery. We can observe how the curves initially start at a voltage slightly below 3 V and drop to lower voltage values as the number of cycles increases. The high voltage value reached by the charging curves in the first few cycles is essentially due to the increase in cycling rate that occurs when moving from the conditioning phase to the stabilization phase. Figure 5b shows the efficiency and discharge capacity trends of the nanostructured battery. The battery reaches a maximum efficiency

value of 88.7% (150th cycle) and then maintains a constant efficiency value around 76.5% throughout its life (Figure 5b).

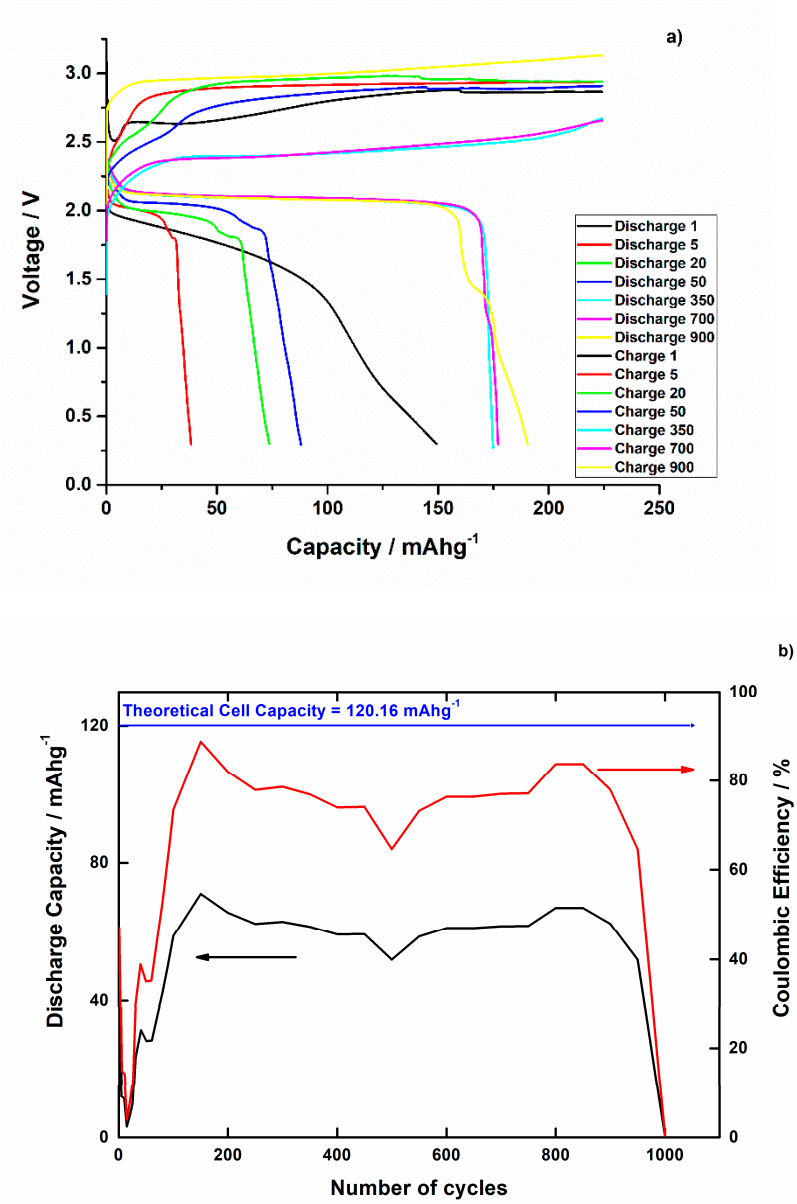

Figure 5. Electrochemical performance of a nanostructured lead-acid battery operating at 25 ± 2 °C and 10 C: (**a**) charging and discharging curves of different cycles, and (**b**) cycling efficiency on discharging and discharge capacity.

Figure 6 show the morphology of the nanostructured Pb (a and b) and PbO_2 (c and d) electrodes after 1000 cycles. The initial nanowire structure is lost due to cyclization, in favor of the formation of lead sulfate crystals. The lead sulfate crystals do not form a compact structure on the electrode surface, but rather form a highly porous structure that allows the electrodes to be subjected to additional high-speed charge and discharge cycles.

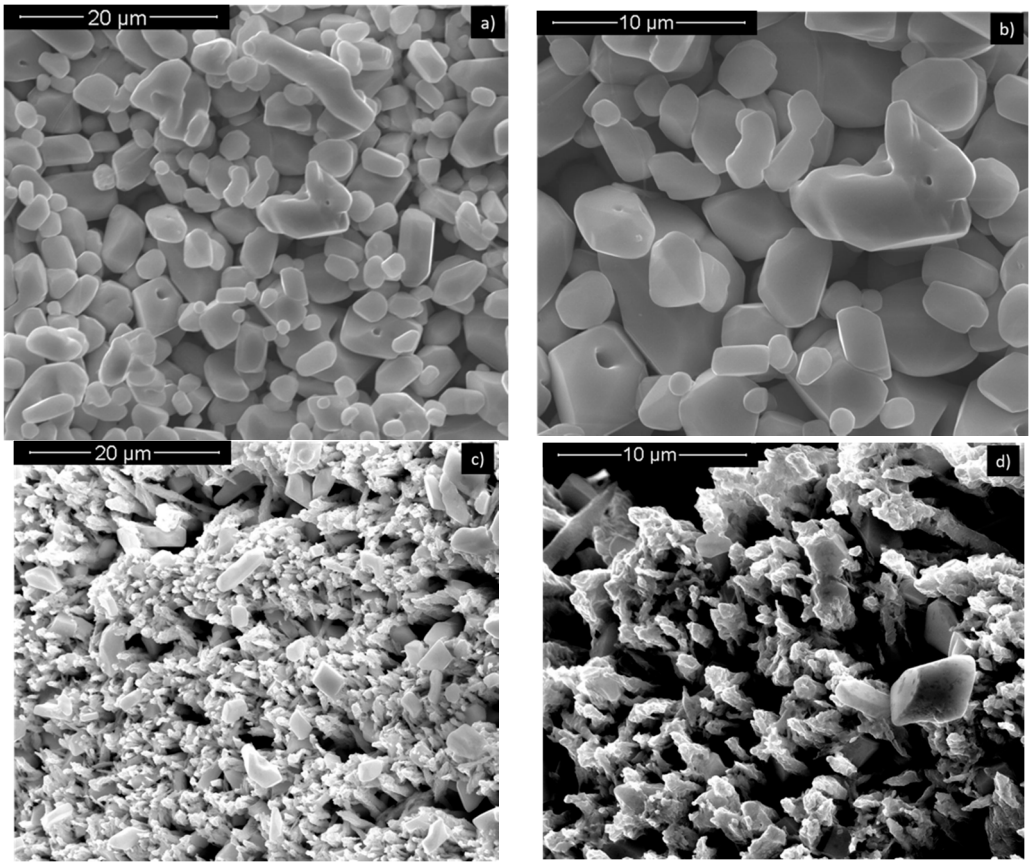

Figure 6. SEM images at different magnifications of Pb and PbO_2 NW electrodes after 1000 cycles at 10 C at the end of the 1000th discharge at 25 ± 2 °C: (**a**,**b**) Pb electrode and (**c**,**d**) PbO_2 electrode.

3.1. Performance of Nanostructured Lead-Acid Electrodes at −20 °C

A VWR cryostat was used to perform the tests at different temperatures. The conditions used were the same as those set for the test of the electrodes at 25 °C: 1.2 V cut-off, a C-rate of 10 C and a total of 1000 charge/discharge cycles. Figure 7 shows the results obtained from cyclization of nanostructured electrodes at a temperature of −20 ± 2 °C.

Figure 7a shows the charge/discharge curves. It can be observed that with the increase of the number of cycles, there was an increase of the plateau of the discharge curve; therefore, there was a greater area under the curve and hence a greater usable energy. From the charge and discharge curves, it can be observed that despite the severe conditions to which the battery has been subjected, from 500° to 1000° cycles, the behavior remains almost unchanged and it is possible to obtain a constant plateau, which means a constant capacity value of the device. The charging curves show a behavior similar to the one shown by the electrodes cycled at 25 °C. In fact, an initial voltage value of about 3.2 V has been measured, probably also in this case due to the rapid variation of the C-rate of the battery, which decreases with the increase of the number of cycles. In contrast to the battery cycled at 25 °C, in this case, the charging curves show the typical pattern of PbO_2 electrodes. At a temperature of −20 °C, an efficiency of about 50% was found, as shown in Figure 7b, compared to a maximum value of 30% found with commercial electrodes [32]. At low temperature, a porous $PbSO_4$ layer is formed which, during charging, is converted into a porous mass of PAM consisting of small particles (<1.5 µm) that agglomerate with each other, forming micropores. This type of structure creates a very large contact surface between the PAM and the electrolyte, ensuring good performance. After testing, both nanostructured electrodes were analyzed by SEM to evaluate their morphological changes. Figure 8a–d show the results of this analysis for both nanostructured electrodes.

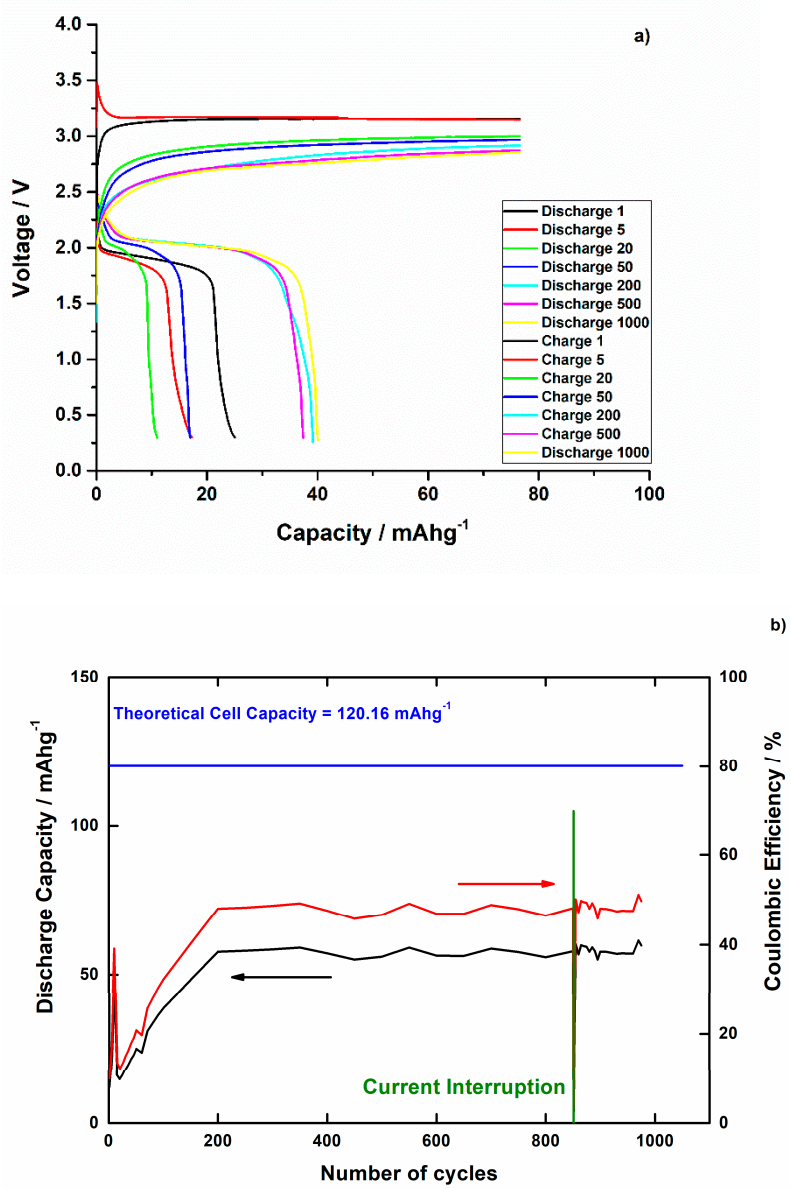

Figure 7. Electrochemical performance of nanostructured lead-acid electrodes operating at −20 ± 2 °C and 10 C: (**a**) charging and discharging curves of different cycles, and (**b**) cycling efficiency on discharging and discharge capacity.

Figure 8a,b show the top view of the Pb nanostructured electrode. The high surface porosity generated by the nanowire cyclization is evident. SEM analysis on the PbO_2 nanostructured electrode is shown in Figure 8c,d. These images show a top view of the PbO_2 nanostructured electrode, and the presence of sulfate agglomerates (of similar shape) with a size of about 10–12 µm distributed all over the surface can be visualized, but in particular, a highly porous surface under the agglomerates can be distinguished.

The observed morphology confirms the trend of the charge and discharge curves reported above and the possibility of a better diffusion of the electrolyte inside the active mass, thus obtaining better performance and longer life times despite the critical conditions to which the electrodes have been exposed.

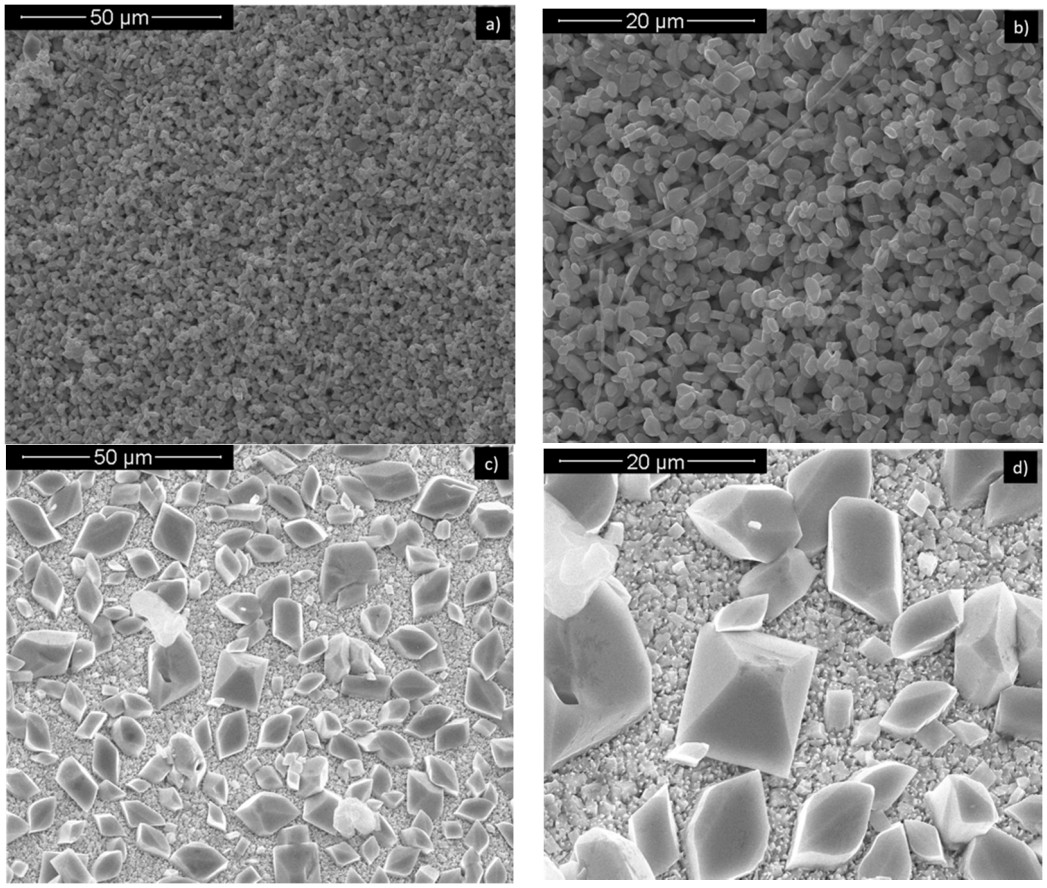

Figure 8. SEM images of Pb and PbO_2 NW electrodes after 1000 cycles at 10 C at the end of the 1000th discharge at -20 ± 2 °C: (**a**,**b**) Pb electrode and (**c**,**d**) PbO_2 electrode.

3.2. Performance of Nanostructured Lead-Acid Electrodes at 40 °C

The tests at 40 ± 2 °C were performed under the same conditions used for the previous tests (Figure 9).

As the number of cycles increases, the plateau of the discharge curve increases. When the 200th cycle is reached, the discharge capacity assumes a constant value, while the discharge curves reach a final voltage of about 2.1 V. Despite that the kinetics of the cell is accelerated by the high temperature, the charge curves do not present any peaks in their trend, which means that even at 40 °C, there is no excessive production of gas at the electrode-electrolyte interface, a phenomenon that could cause the breakage of the electrodes and therefore of the entire battery. The results obtained from the tests showed a battery efficiency of 90%, as shown in Figure 9b. Due to the high temperature, which promotes the reaction kinetics, the nanostructured electrodes reached a high-capacity value that allows them to store more energy than conventional systems under the same operating conditions.

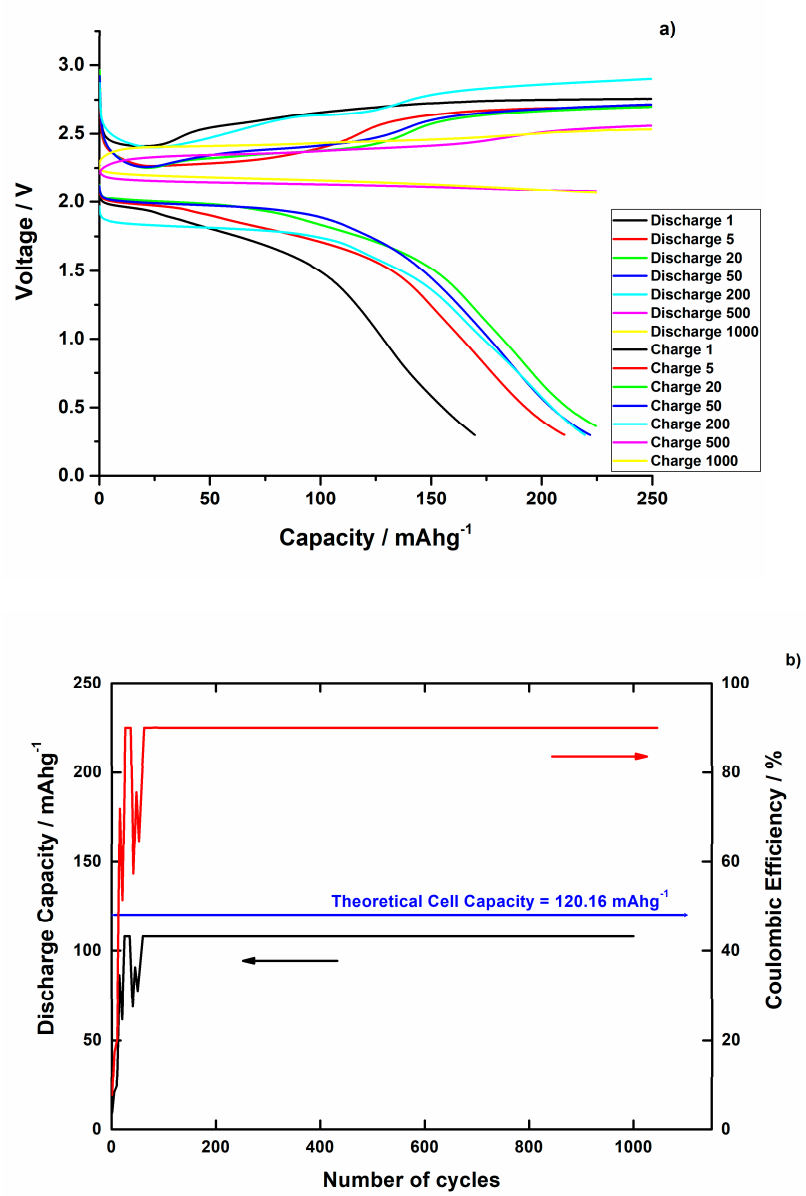

Figure 9. Electrochemical performance of nanostructured lead-acid electrodes operating at 40 ± 2 °C and 10 C: (**a**) charging and discharging curves of different cycles, and (**b**) cycling efficiency on discharging and discharge capacity.

With temperature, the morphology of the electrode changes: at high temperatures, the $PbSO_4$ layer becomes more compact, as reported in the literature [2,33,34]. After testing, both nanostructured electrodes were analyzed by SEM to evaluate their morphology, as shown in Figure 10a–d. The morphology of the Pb nanowires was significantly changed from the original pattern. The absence of nanowires and the presence of large porous agglomerates about 15 µm in size were observed. The morphology of the PbO_2 electrode is shown in Figure 10c,d. The initial NW-shaped morphology was completely lost in favor of the formation of $PbSO_4$ crystals. However, the electrode still has a porous morphology that allows the electrolyte to penetrate the active part and thus allows the battery to operate for further charge and discharge cycles at high C rates.

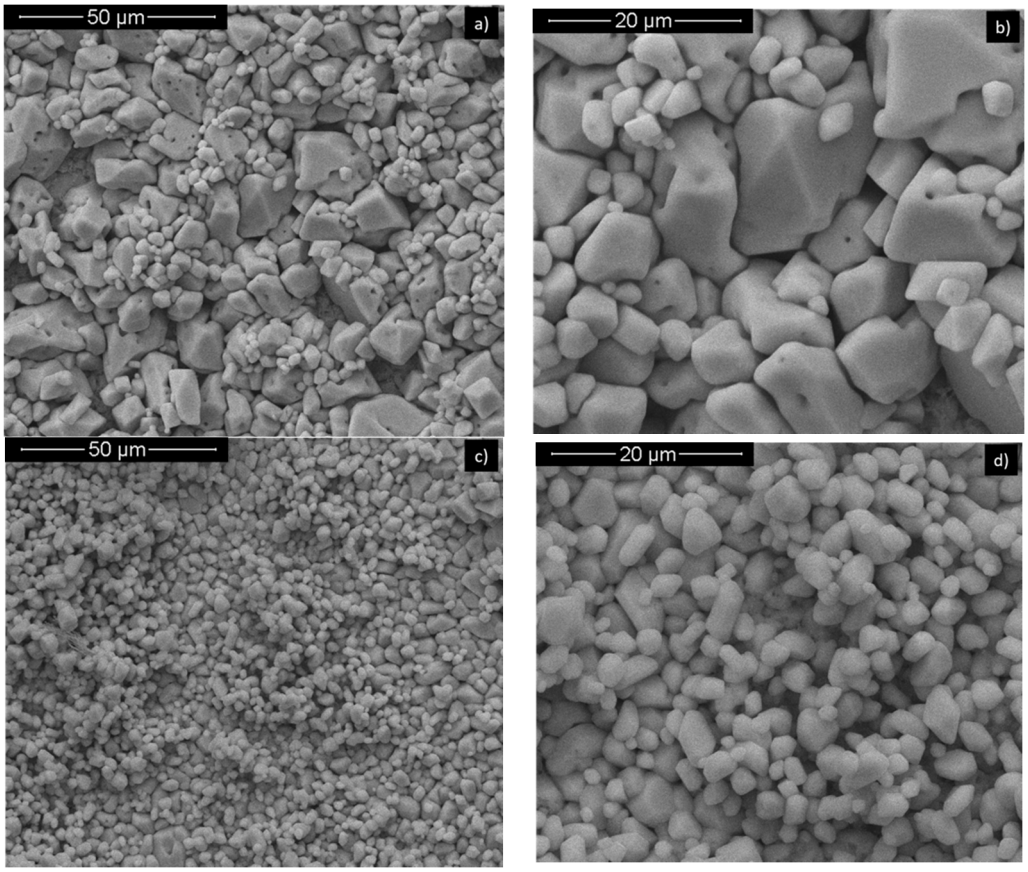

Figure 10. SEM images at different magnifications of Pb and PbO_2 NW electrode after 1000 cycles at 10 C at the end of the 1000th discharge at 40 ± 2 °C: (**a**,**b**) Pb electrode and (**c**,**d**) PbO_2 electrode.

3.3. Comparison of the Results Obtained from Nanostructured Electrodes Cycled at Different Temperatures

Figure 11 shows a comparison of the battery response at different temperatures; in all cases, the 500th cycle was reported. The battery maintained a voltage of below 3 V in all cases, and had no peaks indicating gas production at the electrode surface.

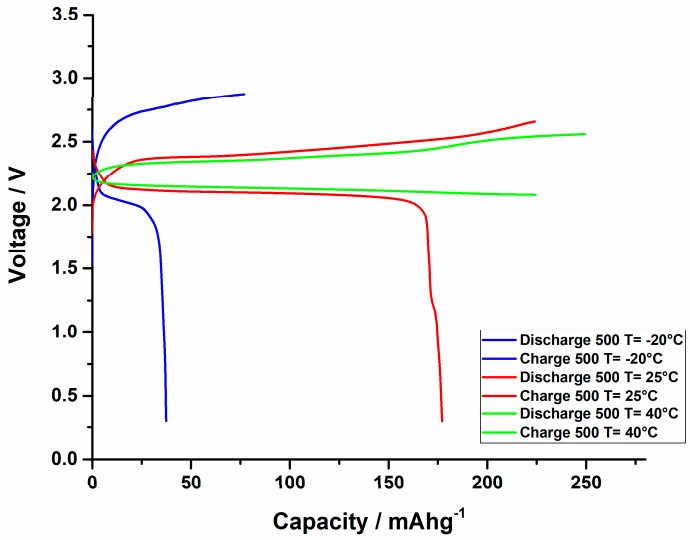

Figure 11. Comparison between charge and discharge curves (500th cycle) at different temperatures.

In the discharge curves, a gradual increase in the plateau of the curves can be seen as the temperature increases. This increase denotes a higher usable energy of the battery, and thus higher efficiency [35]. In particular, for the discharge curve relative to the temperature of 40 ± 2 °C, the cut-off is no longer achieved. This means that the efficiency of this battery has reached 90% and thus all the battery capacity can be converted into usable energy. The discharge curves remained constant over the whole cycling duration at the three temperatures, but different efficiency levels were reached. In particular, battery efficiency increases with temperature, and the maximum efficiency achieved at −20 ± 2 °C was about 50%. This is a very satisfactory result when compared to the maximum efficiency value of conventional lead-acid batteries, which is 30% under optimum operating conditions.

The summarized cyclization results at various temperatures are shown in Table 1. The maximum efficiency increases with temperature; in fact, an efficiency value of 90% was reached at a temperature of 40 ± 2 °C.

Table 1. Performance of nanostructured cells at different temperatures.

Parameter	T = 25 ± 2 °C	T = −20 ± 2 °C	T = 40 ± 2 °C
C-rate	1C (Conditioning phase: complete discharge in 1 h) 10 C (Complete discharge in 6 min)	10 C (Complete discharge in 6 min)	10 C (Complete discharge in 6 min)
Mean Efficiency of discharge	77% at 1 C 88.7% at 10 C	50%	90%
Curves of discharge	Increase of the plateau with number of cycles	Increase of the plateau with number of cycles	Increase of the plateau with number of cycles
Cycle life	>1000	>1000	>1000

Figure 12 shows, for a better comparison, the SEM images of the Pb (Figure 12a–c) and PbO_2 (Figure 12d–f) nanostructured electrodes after testing at different temperatures. In Figure 12a–c, the Pb electrode is shown and the formation of lead sulfate crystals of different sizes is clearly visible on the electrode surface. In particular, there was a decrease in the average grain size with decreasing temperature. However, the post-cycling electrode surface at different temperatures remained highly porous, which allows the electrolyte to penetrate the active mass and the electrodes to be used for further charge/discharge cycles at high C rates.

The post-cycled PbO_2 electrodes, shown in Figure 12d–f, have a widely varying morphology as the operating condition changes. In particular, in Figure 12e, showing a top view of the nanostructured PbO_2 electrode at −20 °C, the presence of sulfate agglomerates (of similar shape) can be observed, with sizes of approximately 10–12 µm distributed over the entire surface, but in particular, a highly porous surface under the agglomerates can be distinguished. The particle size and porosity of lead sulfate is strongly dependent on the discharge conditions, but also temperature, current density, solution concentration and depth of discharge can all affect the lead sulfate crystal structure, leading to a different life cycle.

The result of this morphology confirms the trend of the charge and discharge curves shown above and confirms the possibility of diffusion of the electrolyte within the active mass, thus achieving better performance and longer life times despite the critical conditions to which the batteries have been subjected.

In all analyzed cases, the presence of small sulfate crystals distributed over the entire electrode surface can be observed. From the micrographs of the nanostructured lead and lead oxide electrodes, it can be seen that the formation of lead sulfate on the electrode surface never occurs as a compact layer, but rather as a mixture of granules that ensure a good porosity for the electrode, which allows battery operation above 1000 charge/discharge cycles.

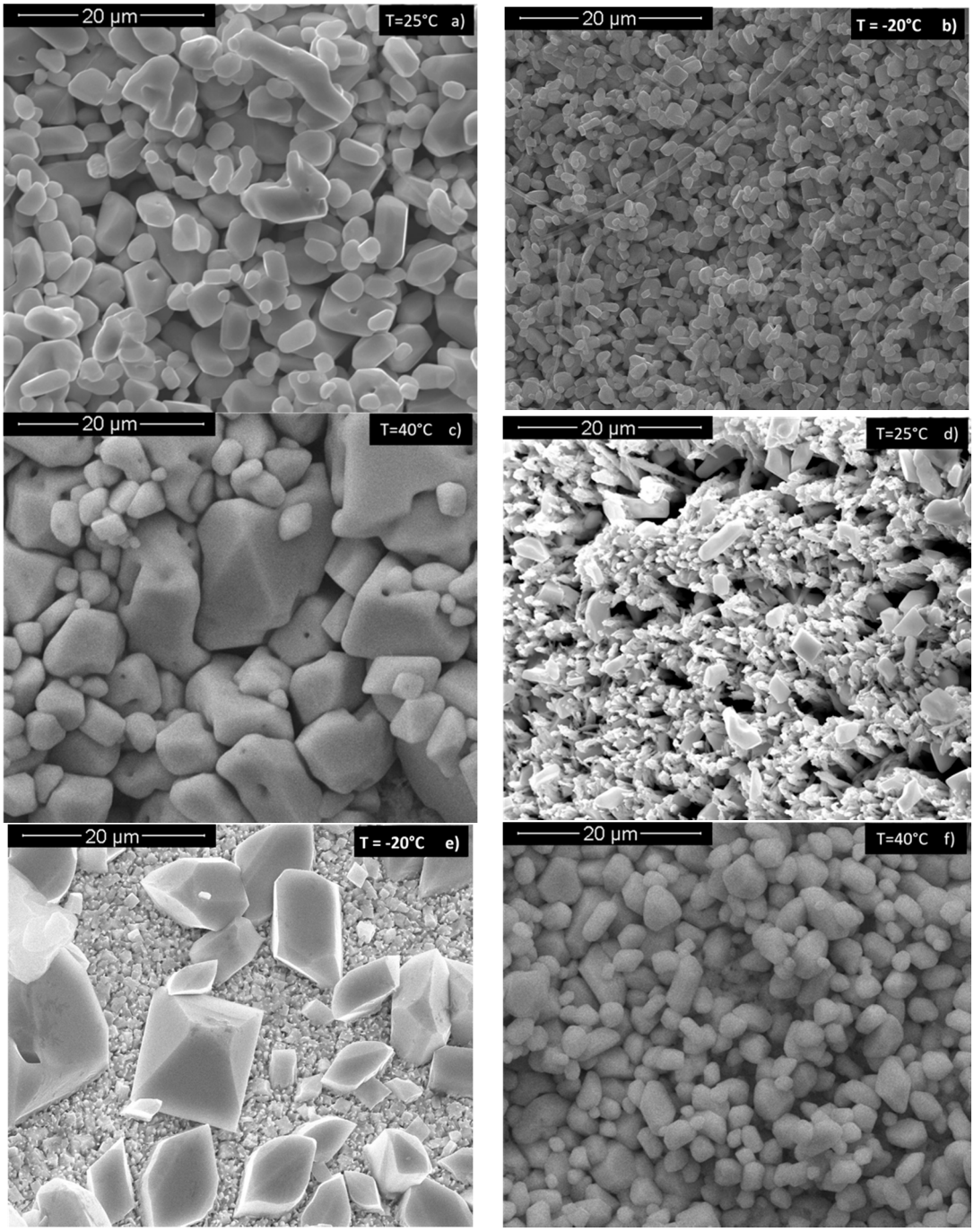

Figure 12. SEM images of Pb and PbO_2 NW electrode after 1000 cycles at 10 C: (**a**) Pb NWs T = 25 ± 2 °C; (**b**) Pb NWs T = −20 ± 2 °C; (**c**) Pb NWs T = 40 ± 2 °C; (**d**) PbO_2 NWs T = 25 ± 2 °C; (**e**) PbO_2 NWs T = −20 ± 2 °C; (**f**) PbO_2 NWs T = 40 ± 2 °C.

4. Conclusions

In this work, the performance of nanostructured lead-acid electrodes has been investigated at different operating temperatures. The results obtained show the potential of this technology in improving the performance of such storage systems, therefore allowing the development of new generations of lead-acid batteries able to overcome the limits of traditional ones.

The nanostructured electrodes have been tested at a rate of 10 C at three different temperatures. In all cases, the nanostructured cell provided excellent results. At a temperature

of 25 °C, the battery reached a mean efficiency value of about 76.5% throughout its lifetime, while at a temperature of 40 °C, an efficiency of 90% was achieved up to over 1000 cycles. The discharge curves showed a plateau that increases with the number of cycles, which results in higher utilizable energy. At temperatures as low as −20 °C, 50% efficiency was obtained, which is higher than conventional lead-acid batteries that reach a maximum of 30% at a lower C rate. Post-cycling morphology of the electrode showed a variegated shape formed by lead sulfate agglomerates of the order of about 10 nm covering the electrode surface. The micrographs showed, mostly for the tests carried out at −20 °C, very small and non-compact structures, characterized by a high porosity that ensures the penetration of the electrolyte in the internal areas, thus ensuring the operation of the nanostructured electrodes for many cycles.

Due to the nanostructured base surface, it has been possible to increase the power density and the battery life, and to improve the efficiency of the system even at a high number of cycles and at critical temperatures.

Author Contributions: Conceptualization, R.L.O., R.I. and G.A.; methodology, M.G.I. and S.P.; software, S.P.; validation, B.P., M.G.I. and S.P.; formal analysis, R.L.O.; investigation, M.G.I. and S.P.; resources, R.I. and G.A.; data curation, S.P.; writing—original draft preparation, R.L.O. and B.P.; writing—review and editing, R.I. and G.A.; supervision, R.I. and G.A.; project administration, R.I.; funding acquisition, R.I. All authors have read and agreed to the published version of the manuscript.

Funding: This research was funded by the University of Palermo and by MIUR grant number POC01_11121.

Data Availability Statement: Data is contained within the article.

Conflicts of Interest: The authors declare no conflict of interest.

References

1. Dong, W.; Dunn, B. Nanomaterials in Energy Storage Systems. In *Nanoscale Materials in Chemistry*; Klabunde, K.J., Richards, R.M., Eds.; John Wiley and Sons: Hoboken, NJ, USA, 2009.
2. Pavlov, D. *Lead-Acid Batteries: Science and Technology a Handbook of Lead-Acid Battery Technology and Its Influence on the Product*; Elsevier: Amsterdam, The Netherlands, 2017.
3. Bode, H. *Lead-Acid Batteries*; Wiley: New York, NY, USA, 1977.
4. Moncada, A.; Mistretta, M.C.; Randazzo, S.; Piazza, S.; Sunseri, C.; Inguanta, R. High-performance of PbO_2 nanowire electrodes for lead-acid battery. *J. Power Surces* **2014**, *256*, 72–79. [CrossRef]
5. Bača, P.; Křivík, P.; Tošer, P.; Vaculík, S. Negative Lead-Acid Battery Electrodes Doped with Glass Fibres. *Int. J. Electrochem. Sci.* **2015**, *10*, 2206–2219.
6. Nanjan, S.; Paul, E.; Steven, W.S.; Dubey, D.P. Lead acid battery performance and cycle life increased through addition of discrete carbon nanotubes to both electrodes. *J. Power Sources* **2015**, *279*, 281–293.
7. Zhu, J.; Hu, G.; Yue, X.; Wang, D. Study of Graphene as a Negative Additive for Valve-Regulated Lead-Acid Batteries Working under HighRate Partial-State-Of-Charge Conditions. *Int. J. Electrochem. Sci.* **2016**, *11*, 700–709.
8. Lankipalli, R.; Manne, V.; Kurivella, S.M.; Mandava, J. Effect of Additives on the Performance of Lead Acid Batteries. *J. Energy Power Eng.* **2015**, *9*, 866–871. [CrossRef]
9. Aleksandrova, A.; Matrakova, M.; Ruecìvski St Nikolov, P.; Pavlov, D. In Proceedings of the Effect of Novel ZnO Additive on the Performance of Lead-Acid Battery Negative Electrod, LABAT'2017, Bulgaria, 14 June 2017. Available online: https://dokumen.tips/reader/f/effect-of-novel-zno-additive-on-the-of-lead-acid-battery-negative-electrode (accessed on 8 July 2021).
10. Battery University. "BU-806a: How Heat and Loading affect Battery Life". 30 May 2019. Available online: http://batteryuniversity.com/index.php/learn/article/how_heat_and_harsh_loading_reduces_battery_life (accessed on 8 July 2021).
11. Diemand, D. *Automotive Batteries at Low Temperatues, in Cold Regions Technical Digest*; Cold Regions Reasearch and Engineering Laboratory: Hanover, NH, USA, 1991.
12. Insinga, M.G.; Oliveri, R.L.; Sunseri, C.; Inguanta, R. Template electrodeposition and characterization of nanostructured Pb as a negative electrode for lead-acid battery. *J. Power Sources* **2019**, *413*, 107–116. [CrossRef]
13. Zubi, G.; Dufo-López, R.; Carvalho, M.; Pasaoglu, G. The lithium-ion battery: State of the art and future perspectives. *Renew. Sustain. Energy Rev.* **2018**, *89*, 292–308. [CrossRef]
14. Xu, W.; Wang, Y. Recent Progress on Zinc-Ion Rechargeable Batteries. *Nano-Micro Lett.* **2019**, *11*, 90. [CrossRef]
15. Tang, B.; Shan, L.; Liang, S.; Zhou, J. Issues and opportunities facing aqueous zinc-ion batteries. *Energy Environ. Sci.* **2019**, *12*, 3288–3304. [CrossRef]
16. Zhu, Y.; Cui, Y.; Alshareef, H.N. An Anode-Free Zn–MnO_2 Battery. *Nano Lett.* **2021**, *21*, 1446–1453. [CrossRef]

17. Fernández, M.; Trinidad, F.; Valenciano, J.; Sánchez, A. Optimization of the cycle life performance of VRLA batteries, working under high rate, partial state of charge (HRPSOC) conditions. *J. Power Sources* **2006**, *158*, 1149–1165. [CrossRef]
18. Snyders, C.; Ferga, E.E.; van Dyl, T. The use of a Polymat material to reduce the effects of sulphation damage occurring in negative electrodes due to the partial state of charge capacity cycling of lead acid batteries. *J. Power Sources* **2012**, *200*, 102–107. [CrossRef]
19. Banerjee, B.Z.; Shilina, Y.; Levi, E.; Luski, S.; Aurbach, D. Single-wall carbon nanotube doping in lead-acid batteries: A new horizon. *Appl. Mater. Interfaces* **2017**, *9*, 3634–3643. [CrossRef]
20. Furukawa1, J.; Smith, K.; Lam, L.T.; Rand, D.A.J. Towards sustainable road transport with the UltraBattery™. In *Lead-Acid Batteries for Future Automobiles*; Garche, J., Karden, E., Moseley, P.T., Rand, D.A.J., Eds.; Elsevier Inc.: Amsterdam, The Netherlands, 2017; pp. 349–391. [CrossRef]
21. Büngeler, J.; Cattaneo, E.; Riegel, B.; Sauer, D.U. Advantages in energy efficiency of flooded lead-acid batteries when using partial state of charge operation. *J. Power Sources* **2018**, *375*, 53–58. [CrossRef]
22. Insinga, M.G.; Moncada, A.; Oliveri, R.L.; Ganci, F.; Piazza, S.; Sunseri, C.; Inguanta, R. Nanostructured Pb electrode for innovative leadacid battery. *Chem. Eng. Trans.* **2017**, *60*, 49–54.
23. Caruso, M.; Castiglia, V.; Miceli, R.; Nevoloso, C.; Romano, P.; Schettino, G.; Viola, F.; Insinga, M.; Moncada, A.; Oliveri, R.; et al. Nanostructured lead acid battery for electric vehicles applications. In Proceedings of the 2017 International Conference of Electrical and Electronic Technologies for Automotive, Turin, Italy, 15–16 June 2017. [CrossRef]
24. Inguanta, R.; Rinaldo, E.; Piazza, S.; Sunseri, C. Lead nanowires for microaccumulators obtained through indirect electrochemical template deposition. *Electrochem. Solid-State Lett.* **2009**, *13*, K1–K4. [CrossRef]
25. Inguanta, R.; Piazza, S.; Sunseri, C.; Cino, A.; Di Dio, V.; LA Cascia, D.; Miceli, R.; Rando, C.; Zizzo, G. An electrochemical route towards the fabrication of nanostructured semiconductor solar cells. *SPEEDAM 2010* **2010**, *5542264*, 1166–1171. [CrossRef]
26. Inguanta, R.; Ferrara, G.; Piazza, S.; Sunseri, C. Nanostructures fabrication by template deposition into anodic alumina membranes. *Chem. Eng. Trans.* **2008**, *17*, 957–962.
27. Battaglia, M.; Inguanta, R.; Piazza, S.; Sunseri, C. Fabrication and characterization of nanostructured Ni-IrO_2 electrodes for water electrolysis. *Int. J. Hydrog. Energy* **2014**, *39*, 16797–16805. [CrossRef]
28. Ganci, F.; Lombardo, S.; Sunseri, C.; Inguanta, R. Nanostructured electrodes for hydrogen production in alkaline electrolyzer. *Renew. Energy* **2018**, *123*, 117–124. [CrossRef]
29. Linden, D.; Reddy, T.B. (Eds.) *Handbook of Batteries*, 4th ed.; McGraw-Hill: New York, NY, USA, 2010.
30. Boudieb, N.; Bounoughaz, M.; Nazef-Allaoua, M. Influence of Surfactant as an Electrolyte Additive on the Electrochemical and Corrosion Behaviors of Lead-Acid Battery. University M'Hamed Bougara-UMBB-Boumerdes, Faculty of Engineering Science, Laboratory of Polymers Treatment and Forming; Avenue of Independence–Boumedes-35000-Algeria. Department of Corrosion, Development & Technologies Division, Upstream Activity, Sonatrach2 1th November Avenue, Boumedes-35000 ALGERIA. Available online: https://www.semanticscholar.org/paper/Influence-of-surfactant-as-an-electrolyte-additive-Boudieb-Bounoughaz/92d3833f682fd4bb7fa15ecb2c1f1f09e9d4e769 (accessed on 8 July 2021).
31. Secondary Cells and Batteries for Renewable Energy Storage—General Requirements and Methods of test—Part 1: Photovoltaic off-Grid Application. BSI Standards Publication: BS EN 61427-1:2013. Available online: https://www.thenbs.com/PublicationIndex/documents/details?Pub=BSI&DocID=305840 (accessed on 8 July 2021).
32. Insinga, M.G.; Pisana, S.; Oliveri, R.L.; Sunseri, C.; Inguanta, R. *Performance of Lead-Acid Batteries with Nanostructured Electrodes at Different Temperature*; IEEE: New York, NY, USA, 2018. [CrossRef]
33. Hutchinson, R. *Temperature Effects on Sealed Lead Acid Batteries and Charging Techniques to Prolong Cycle Life*; Sandia National Laboratories: Albuquerque, NM, USA, 2004.
34. Budevski, E.; Staikov, G.; Lorenz, W.J. Electrocrystallization Nucleation and growth phenomena. *Electrochim. Acta* **2000**, *45*, 2559–2574. [CrossRef]
35. Rodríguez-Sánchez, L.; Blanco, A.M.C.; López-Quintela, M.A. Electrochemical Synthesis of Silver Nanoparticles. *J. Phys. Chem. B* **2000**, *104*, 9683–9688. [CrossRef]